

## High-Capacity Hydrogen and Nitric Oxide Adsorption and Storage in a Metal–Organic Framework

Bo Xiao,<sup>†</sup> Paul S. Wheatley,<sup>†</sup> Xuebo Zhao,<sup>‡</sup> Ashleigh J. Fletcher,<sup>‡</sup> Sarah Fox,<sup>||</sup> Adriano G. Rossi,<sup>||</sup> Ian L. Megson,<sup>§</sup> S. Bordiga,<sup>⊥</sup> L. Regli,<sup>⊥</sup> K. Mark Thomas,<sup>\*,‡</sup> and Russell E. Morris<sup>\*,†</sup>

*Contribution from the EaStChem School of Chemistry, University of St. Andrews, Purdie Building, St. Andrews KY16 9ST, United Kingdom, Northern Carbon Research Laboratories, School of Natural Sciences, Bedson Building, University of Newcastle upon Tyne, Newcastle upon Tyne NE1 7RU, United Kingdom, Free Radical Research Facility, UHI Millennium Institute, Inverness IV2 3BL, United Kingdom, Queen's Medical Research Institute, University of Edinburgh, 47 Little France Crescent, Edinburgh EH16 4TJ, United Kingdom, Dipartimento di Chimica IFM and NIS Centre of Excellence, Univeristà di Torino, Via P. Giuria 7, I-10125 Torino, Italy*

Received August 22, 2006; E-mail: mark.thomas@newcastle.ac.uk; rem1@st-and.ac.uk

**Abstract:** Gas adsorption experiments have been carried out on a copper benzene tricarboxylate metal–organic framework material, HKUST-1. Hydrogen adsorption at 1 and 10 bar (both 77 K) gives an adsorption capacity of 11.16 mmol H<sub>2</sub> per g of HKUST-1 (22.7 mg g<sup>-1</sup>, 2.27 wt %) at 1 bar and 18 mmol per g (36.28 mg g<sup>-1</sup>, 3.6 wt %) at 10 bar. Adsorption of D<sub>2</sub> at 1 bar (77 K) is between 1.09 (at 1 bar) and 1.20 (at <100 mbar) times the H<sub>2</sub> values depending on the pressure, agreeing with the theoretical expectations. Gravimetric adsorption measurements of NO on HKUST-1 at 196 K (1 bar) gives a large adsorption capacity of ~9 mmol g<sup>-1</sup>, which is significantly greater than any other adsorption capacity reported on a porous solid. At 298 K the adsorption capacity at 1 bar is just over 3 mmol g<sup>-1</sup>. Infra red experiments show that the NO binds to the empty copper metal sites in HKUST-1. Chemiluminescence and platelet aggregometry experiments indicate that the amount of NO recovered on exposure of the resulting complex to water is enough to be biologically active, completely inhibiting platelet aggregation in platelet rich plasma.

### Introduction

Porous materials of many different kinds<sup>1</sup> continue to be at the forefront of attempts to develop many emerging technologies; in particular, gas adsorption properties of porous materials are currently receiving great interest in many areas of science. Potential uses of these solids range from separations of mixtures to gas storage media for energy,<sup>2</sup> environmental,<sup>3</sup> and biological applications.<sup>4</sup> Metal–organic frameworks (MOFs), with their extremely high surface areas and porosity and their varied

chemical compositions, are good candidates for high adsorption capacities of various gases. HKUST-1 is a copper benzene tricarboxylate porous material first reported by Williams and co-workers<sup>5</sup> and subsequently studied by numerous research groups. Perhaps the most interesting feature of this material is the presence of a metal site in the walls of the material that, after dehydration, is potentially available to act as a site where coordination to a gas molecule can take place.

Hydrogen adsorption and storage is of great interest as a method of providing the gas as a fuel for zero-emission energy production. The approaches currently being adopted for the design of hydrogen storage materials are based on many different types of material, ranging from metal hydrides<sup>6</sup> and carbon nanotubes and nanohorns<sup>7</sup> to gas clathrates,<sup>8</sup> although all have significant problems attached to them. Nanoporous materials, with their inherently large internal pore volumes and

<sup>†</sup> University of St. Andrews.

<sup>‡</sup> University of Newcastle upon Tyne.

<sup>§</sup> Free Radical Research Facility, UHI Millennium Institute.

<sup>||</sup> University of Edinburgh.

<sup>⊥</sup> Univeristà di Torino.

- (1) (a) Davis, M. E. *Nature* **2002**, *417*, 813. (b) Corma, A.; Diaz-Cabanas, M.; Jorda, J. L.; Martinez, C.; Moliner, M. *Nature* **2006**, *443*, 842. (c) Cooper, E. R.; Andrews, C. D.; Wheatley, P. S.; Webb, P. B.; Wormald, P.; Morris, R. E. *Nature* **2004**, *430*, 1012.
- (2) (a) Eddaoudi, M.; Kim, J.; Rosi, N.; Vodak, D.; Wachter, J.; O'Keefe, M.; Yaghi, O. M. *Science* **2002**, *295*, 469. (b) Rosi, N. L.; Eckert, J.; Eddaoudi, M.; Vodak, D.; Kim, J.; O'Keefe, M.; Yaghi, O. M. *Science* **2003**, *300*, 1127. (c) Zhao, X.; Xiao, B.; Fletcher, A. J.; Thomas, K. M.; Bradshaw, D.; Rosseinsky, M. J. *Science* **2004**, *306*, 1012. (d) Ferey, G.; Mellot-Draznieks, C.; Serre, C.; Millange, F.; Dutour, J.; Surble, S.; Margiolaki, I. *Science* **2005**, *309*, 2040.
- (3) Millward, A. R.; Yaghi, O. M. *J. Am. Chem. Soc.* **2005**, *127*, 17998.
- (4) Wheatley, P. S.; Butler, A. R.; Crane, M. S.; Fox, S.; Xiao, B.; Rossi, A. G.; Megson, I. L.; Morris, R. E. *J. Am. Chem. Soc.* **2006**, *128*, 502.
- (5) Chui, S. S. Y.; Lo, S. M. F.; Charmant, J. P. H.; Orpen, A. G.; Williams, I. D. *Science* **1999**, *283*, 1148.

(6) (a) Schlapbach, L.; Züttel, A.; *Nature* **2001**, *414*, 353. (b) Bogdanovic, B.; Felderhoff, M.; Pommerin, A.; Schuth, T.; Spielkamp, N. *Adv. Mater.* **2006**, *18*, 1998.

(7) (a) Dillon, A. C.; Jones, K. M.; Bekkedahl, T. A.; Kiang, C. H.; Bethune, D. S.; Heben, M. J. *Nature* **1997**, *386*, 377. (b) Zhou, Y.; Feng, K.; Sun, Y.; Zhou, L. *Chem. Phys. Lett.* **2003**, *380*, 526. (c) Shiraishi, M.; Takenobu, T.; Kataura, H.; Ata, M. *Appl. Phys.* **2004**, *A78*, 947. (d) H. Kanoh, H.; Yudasaka, M.; Iijima, S.; Kaneko, K. *J. Am. Chem. Soc.* **2005**, *127*, 7511.

(8) Lee, H.; Lee, J. W.; Kim, D. Y.; Park, J.; Seo, Y. T.; Zeng, H.; Moudrakovski, I. L.; Ratcliffe, C. I.; Ripmeester, J. A. *Nature* **2005**, *434*, 743.

surface areas are obvious candidates for high-capacity storage materials. MOFs have great promise in this area, and HKUST-1 has been shown to be capable of adsorbing significant amounts of hydrogen at 77 K. There are, however, significant questions still to be answered. From the literature it is clear that, while hydrogen adsorption capacity is still usually below the levels required for commercial application, high-capacity materials are being prepared. The relatively weak interaction between the hydrogen molecule and the walls of porous solids means that this adsorption is only significant at low temperatures, which might further limit the possible applications.

High nitric oxide (NO) adsorption is of great interest for environmental applications in gas separation and NO<sub>x</sub> traps for lean burn engines. NO is also an extremely important molecule in biology, and NO-storing solids have potential applications as antithrombosis materials.<sup>9</sup> NO is a crucial biological agent in the cardiovascular, nervous, and immune systems.<sup>10</sup> NO synthesized by endothelial cells that line blood vessels mediates a number of vital functions, including vasodilation<sup>11,12</sup> and inhibition of platelet<sup>13</sup> and inflammatory cell<sup>14,15</sup> activation and adhesion. In addition, NO is an important neurotransmitter and neuromodulator in the peripheral and central nervous systems,<sup>16</sup> and its synthesis in high concentrations contributes to the cytotoxic effects of inflammatory cells on invading pathogens.<sup>17</sup>

The delivery of exogenous NO is an attractive therapy for a number of ailments, but the range and diversity of its effects make target specificity a major concern, which has held back the development of some NO applications. To overcome this problem requires the development of materials that can store significant quantities of NO and then deliver it to specific sites in the body. There is currently particular interest in using NO delivery materials to prevent life-threatening complications associated with thrombosis formation at the surface of medical devices such as stents and catheters.<sup>9</sup>

A number of materials have been proposed as delivery agents for exogenous NO. Perhaps the chemically most advanced are those based on polymers or silica functionalized with secondary amines, which, on reaction with NO, form ionic diazeniumdiolates that can be used to increase the thromboresistivity of polymers.<sup>9,18,19</sup> Two molecules of NO react with each amine (giving rise to the trivial name NONOate) and are released on contact with moisture at an appropriate pH. Other methods of release have also been explored, including the light-activated

release of nitric oxide from metal containing polymers.<sup>20</sup> More recently zeolites, nanoporous inorganic framework materials normally associated with the destruction of NO in deNO<sub>x</sub> catalysis, have also been shown to be high-storage capacity materials for NO, with maximum adsorption capacities of around 1 mmol g<sup>-1</sup> at 298 K.<sup>4</sup>

A specific potential use for NO-releasing materials in the cardiovascular arena centers on the prevention of thrombosis on artificial surfaces that come into contact with blood, particularly in relation to procedures that require extracorporeal circuits, such as bypass and renal replacement therapy, catheter implantations, or stents that are used in interventional cardiology to improve the patency of partially blocked arteries.<sup>9</sup> Current best practice to prevent thrombosis in these situations involves the administration of heparin, other anticoagulants, or antiplatelet agents to the patient, with the inherent risk of hemorrhagic<sup>21,22</sup> or paradoxical thrombotic<sup>23</sup> complications. Stent coatings that release antithrombotic,<sup>24,24</sup> antiinflammatory,<sup>25</sup> and antimitogenic<sup>26</sup> agents to reduce in-stent thrombosis or restenosis have met with some success, but NO might be expected to have all of these effects if delivered at the appropriate rate for a sufficient duration. Other potential uses of these types of solid, as shown by a number of different biological effects, include antibacterial coatings<sup>27</sup> and wound-healing promoters.<sup>28</sup>

Here we report the full characterization of the porous nature of HKUST-1 using N<sub>2</sub> and CO<sub>2</sub> adsorption together with a demonstration of high H<sub>2</sub> and D<sub>2</sub> adsorption. We also show that HKUST-1 adsorbs significantly more NO than any other porous solid yet reported and that it releases enough NO on contact with a physiological solution (platelet-rich plasma) to fully inhibit platelet aggregation.

## Results and Discussion

**Hydrogen Adsorption Studies.** HKUST-1 was synthesized according to the method reported by Williams and co-workers.<sup>5</sup> The powder X-ray diffraction pattern indicated that there were none of the impurities reported in the initial publications. Nitrogen (77 K) and carbon dioxide (195 K) adsorption studies were used to characterize the pore volume in the material, giving values of 0.684 and 0.703 cm<sup>3</sup> g<sup>-1</sup>, respectively. Pore volumes of HKUST-1 obtained from N<sub>2</sub> adsorption have been reported as 0.33 cm<sup>3</sup> g<sup>-1</sup> by Chui et al.<sup>5</sup> and 0.4 cm<sup>3</sup> g<sup>-1</sup> in Lee's paper;<sup>29</sup>

- (9) Keefer, L. K. *Nat. Mater.* **2003**, *2*, 357.  
 (10) Moncada, S.; Palmer, R. M. J.; Higgs, E. A. *Pharmacol. Rev.* **1991**, *43*, 109.  
 (11) Furchgott, R. F.; Zawadzki, J. V. *Nature* **1980**, *288*, 373.  
 (12) Palmer, R. M. J.; Ferrige, A. G.; Moncada, S. *Nature* **1987**, *327*, 524.  
 (13) Radomski, M. W.; Palmer, R. M. J.; Moncada, S. *Lancet* **1987**, *2*, 1057.  
 (14) Bath, P. M. W.; Hassall, D. G.; Gladwin, A. M.; Palmer, R. M. J.; Martin, J. F. *Arterioscler. Thromb.* **1991**, *11*, 254.  
 (15) Kubes, P.; Suzuki, M.; Granger, D. N. *Proc. Natl. Acad. Sci. U.S.A.* **1991**, *87*, 5193.  
 (16) Garthwaite, J. *Trends Neurosci.* **1991**, *14*, 60.  
 (17) Nathan, C. F.; Hibbs, J. B. *Curr. Opin. Immunol.* **1991**, *3*, 65.  
 (18) (a) Parzuchowski, P. G.; Frost, M. C.; Meyerhoff, M. E. *J. Am. Chem. Soc.* **2002**, *124*, 12182. (b) Lee, Y.; Oh, B. K.; Meyerhoff, M. E. *Anal. Chem.* **2004**, *76*, 536. (c) Zhang, H. P.; Annich, G. M.; Miskulin, J.; Stankiewicz, K.; Osterholzer, K.; Merz, S. I.; Bartlett, R. H.; Meyerhoff, M. E. *J. Am. Chem. Soc.* **2003**, *125*, 5015. (d) Frost, M. C.; Rudich, S. M.; Zhang, H. P.; Maraschio, M. A.; Meyerhoff, M. E. *Anal. Chem.* **2002**, *74*, 5942. (e) Zhang, H. P.; Annich, G. M.; Miskulin, J.; Osterholzer, K.; Merz, S. I.; Bartlett, R. H.; Meyerhoff, M. E. *Biomaterials* **2002**, *23*, 1485.  
 (19) (a) Mowery, K. A.; Schoenfish, M. H.; Saavedra, J. E.; Keefer, L. K.; Meyerhoff, M. E. *Biomaterials* **2000**, *21*, 9. (b) Mowery, K. A.; Schoenfish, M. H.; Baliga, N.; Wahr, J. A.; Meyerhoff, M. E. *Electroanalysis* **1999**, *11*, 681. (c) Espadas-Torre, C.; Oklejas, V.; Mowery, K.; Meyerhoff, M. E. *J. Am. Chem. Soc.* **1997**, *119*, 2321.

- (20) (a) Mitchell-Koch, J. T.; Reed, T. M.; Borovik, A. S. *Angew. Chem.* **2004**, *43*, 2806. (b) Padden, K. M.; Krebs, J. F.; MacBeth, C. E.; Scarrow, R. C.; Borovik, A. S. *J. Am. Chem. Soc.* **2001**, *123*, 1072.  
 (21) Sundlof, D. W.; Rerkpattanapit, P.; Wongpraparut, N.; Pathi, P.; Kotler, M. N.; Jacobs, L. E.; Ledley, G. S.; Yazdanfar, S. *Am. J. Cardiol.* **1999**, *83*, 1569.  
 (22) Bennett, C. L.; Connors, J. M.; Carwile, J. M.; Moake, J. L.; Bell, W. R.; Tarantolo, S. R.; McCarthy, L. J.; Sarode, R.; Hatfield, A. J.; Feldman, M. D.; Davidson, C. J.; Tsai, H. M. *N. Engl. J. Med.* **2000**, *342*, 1773.  
 (23) Chong, B. H. *J. Thromb. Haemostasis* **2003**, *1*, 1471.  
 (24) Aggarwal, R. K.; Martin, W. A.; Azrin, M. A.; Ezekowitz, M. D.; de Bono, D. P.; Gershlick, A. H. *Circulation* **1996**, *94*, 1510.  
 (25) Strecker, E. P.; Gabelmann, A.; Boos, I.; Lucas, C.; Xu, Z. Y.; Haberstroh, J.; Freudenberg, N.; Stricker, H.; Langer, M.; Betz, E. *Cardiovasc. Intervent. Radiol.* **1998**, *21*, 487.  
 (26) Colombo, A.; Drzewiecki, J.; Banning, A.; Grube, E.; Hauptmann, G.; Silber, S.; Dudek, D.; Fort, S.; Schiele, F.; Zmudka, K.; Guagliumi, G.; Russell, M. E. *Circulation* **2003**, *108*, 788.  
 (27) Nablo, B. J.; Chen, T.-Y.; Schoenfish, M. H. *J. Am. Chem. Soc.* **2001**, *123*, 9712.  
 (28) Shabani, M.; Pulfer, S. K.; Bulgrin, J. P.; Smith, D. J. *Wound Rep. Regen.* **1996**, *4*, 353.  
 (29) Lee, J.-Y.; Li, J.; Jagiello, J. *J. Solid State. Chem.* **2005**, *178*, 2527.

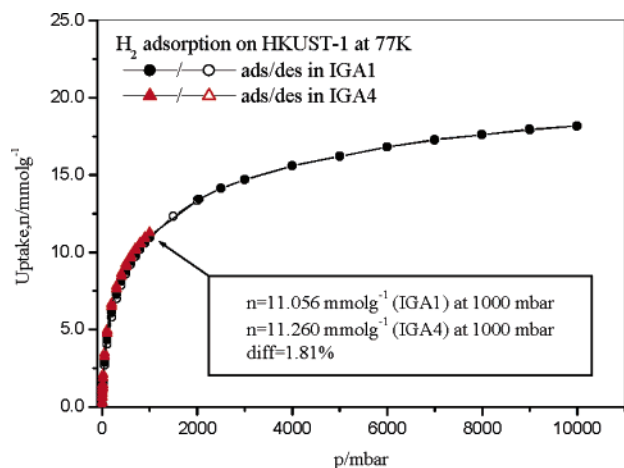


**Figure 1.** Adsorption and desorption isotherms (77 K) for H<sub>2</sub> on HKUST-1 to 1 bar (red triangles) and to 10 bar (black circles). The repeatability is <2% at 1 bar. IGA1 and IGA4 are different instruments for high- and low-pressure measurements respectively.

Rowell et al.<sup>31</sup> reported a value of 0.75 cm<sup>3</sup> g<sup>-1</sup>. The calculated crystallographic pore volume obtained from PLATON is ~0.72 cm<sup>3</sup> g<sup>-1</sup>.

Highly crystalline materials such as HKUST-1 should have very repeatable pore structures and adsorption properties, but reports of hydrogen adsorption properties of HKUST-1 vary quite substantially. Lee et al.<sup>29</sup> and Prestipino et al.<sup>30</sup> both report a H<sub>2</sub> uptake of ~6 mmol g<sup>-1</sup> (~12.5 mg g<sup>-1</sup>, ~1.25 wt %), while Yaghi and co-workers report 12.4 mmol g<sup>-1</sup> (25 mg g<sup>-1</sup>, 2.5 wt %)<sup>31</sup> in one paper and nearer 7.9 mmol g<sup>-1</sup> (16 mg g<sup>-1</sup>, 1.6 wt %)<sup>32</sup> in another (all measurements 77 K and 1 bar. Note that the result from ref 32 is based on interpolation of a high-pressure isotherm). The issues with regard to repeatability of nitrogen adsorption measurements for HKUST-1 may be attributed to (1) sample purity and (2) sample activation. The presence of amorphous or nonporous impurity phases must be eliminated. Activation involves removal of any guest molecules that are contained within the pores of the material, either through thermal or chemical means (or through a combination of the two). The stage where the template has been completely removed by evacuation to give the porous structure has to be established carefully. Good agreement between pore volumes obtained from crystallographic studies and gas adsorption is necessary to confirm the purity of the material. In the case of H<sub>2</sub> adsorption measurements, there are additional considerations since the experimental system must be ultraclean and it is necessary to purify even ultrahigh-purity hydrogen before the measurements.

Several hydrogen adsorption experiments were repeated using samples of HKUST-1 from different batches and different adsorption instruments and to pressures of 1 and 10 bar (77 K). We have carefully characterized the buoyancy corrections needed, and the repeatability of the results gives us great confidence that the sample- and instrument-dependent factors have been controlled (See Supporting Information).

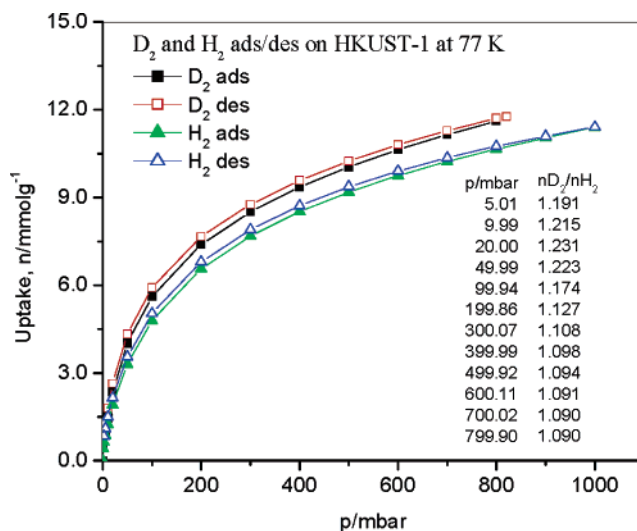


**Figure 2.** H<sub>2</sub> and D<sub>2</sub> adsorption desorption isotherms (77 K to 1 bar) on HKUST-1. The D<sub>2</sub>/H<sub>2</sub> ratio of adsorption at 800 mbar is 1.09.

Gravimetric measurements at 1 bar indicate an average H<sub>2</sub> adsorption capacity of ~11.16 mmol g<sup>-1</sup> of HKUST-1 (22.7 mg g<sup>-1</sup>, 2.27 wt %, Figure 1) comparable to the highest results reported by Yaghi and co-workers.<sup>31</sup> The isotherm is repeatable to within 1.8% on different instruments and using different samples of HKUST-1. At higher pressure (10 bar) the adsorption capacity increases up to approximately 18 mmol per g (36.28 mg g<sup>-1</sup>, 3.6 wt % Figure 1). Yaghi and co-workers<sup>32</sup> reported the adsorption isotherms up to 80 bar as only 16.17 mmol g<sup>-1</sup> (32.6 mg g<sup>-1</sup>, 3.26 wt %). D<sub>2</sub> adsorption on HKUST-1 at 77 K up to 1 bar (Figure 2) shows a slight increase in adsorption capacity (from 1.09 to 1.20 times the H<sub>2</sub> values depending on the pressure). This is consistent with adsorption studies on porous carbons<sup>33</sup> and zeolites<sup>34</sup> and is due to quantum mechanical effects. The density of the adsorbed hydrogen calculated from the maximum amount adsorbed determined using the Langmuir equation and the N<sub>2</sub> pore volume was ~0.057 g cm<sup>-3</sup>. This value is similar to densities for porous carbons and lower than 0.0708 g cm<sup>-3</sup> for liquid H<sub>2</sub> at 20.2 K.<sup>35</sup>

These results show that the maximum adsorption capacity of HKUST-1 for hydrogen at 77 K was 11.16 mmol g<sup>-1</sup>, or approximately 2.27 wt % at 1 bar rising to approximately 18 mmol g<sup>-1</sup> at 10 bar. None of the samples we measured showed the lower adsorption capacities reported by Lee et al. and Prestipino et al.

### Nitric Oxide Adsorption Studies

Nitric oxide adsorption is important for a number of applications, with particular potential for impact in the medical and biological areas. Materials based on organic<sup>19</sup> and metal-containing polymers,<sup>21</sup> and zeolites<sup>4</sup> have all been proposed as NO adsorbents. The adsorption capacity of these materials ranges from quite low values in the μmol NO per g range<sup>21</sup> up to approximately 1 to 1.5 mmol NO per g of material.<sup>4,19</sup> Although adsorption capacity is not the only consideration in

(30) Prestipino, C.; Regli, L.; Vitillo, J. G.; Bonino, F.; Damin, A.; Lamberti, C.; Zecchina, A.; Solari, P. L.; Kongshaug, K. O.; Bordiga, S. *Chem. Mater.* **2006**, *18*, 1337.

(31) Rowell, J. L. C.; Yaghi, O. M. *J. Am. Chem. Soc.* **2006**, *128*, 1304.

(32) Wong-Foy, A. G.; Matzger, A. J.; Yaghi, O. M. *J. Am. Chem. Soc.* **2006**, *128*, 3494.

(33) (a) Zhao, X. B.; Xiao, B.; Fletcher, A. J.; Thomas, K. M. *J. Phys. Chem. B* **2005**, *109*, 8880. (b) Zhao, X. B.; Villar-Rodil, S.; Fletcher, A. J.; Thomas, K. M. *J. Phys. Chem. B* **2006**, *110*, 9947.

(34) Stephanie-Victoire, F.; Goulay, A. M.; de Lara, E. C. *Langmuir* **1998**, *14*, 7255.

(35) *CRC Handbook of Chemistry and Physics*, 74th ed.; CRC Press: Boca Raton, Florida, 1993.

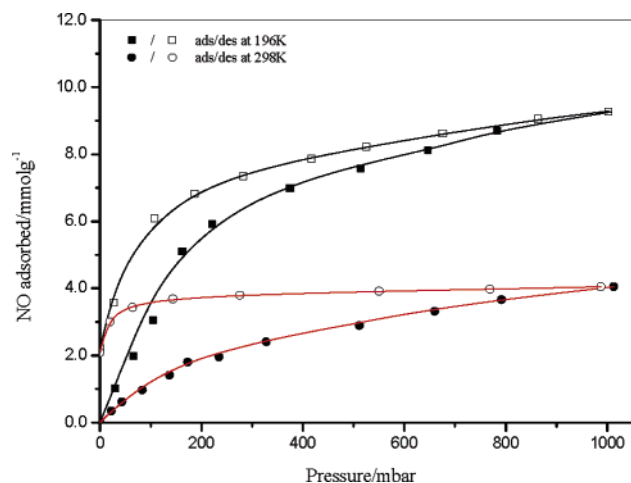


**Figure 3.** Adsorption (filled symbols) and desorption (open symbols) isotherms at 196 K (squares) and 298 K (circles) for nitric oxide on HKUST-1.

determining the effectiveness of a material, it is advantageous to maximize the adsorption capacity of a material to increase the reservoir of stored gas. NO is physisorbed in the pores and also coordinates with the metal sites present in HKUST-1. Gravimetric adsorption measurements on HKUST-1 at 196 K (1 bar) gives a large adsorption capacity of  $\sim 9$  mmol  $g^{-1}$ , which is significantly greater than any other adsorption capacity reported on a porous solid. At 298 K the adsorption capacity at 1 bar is just over 3 mmol  $g^{-1}$ . These values are high, bearing in mind that the NO critical temperature and pressure are 180.1 K and 64.83 bar. There is significant isotherm hysteresis at both temperatures, indicative of the strong irreversible adsorption of some of the NO molecules on the open copper sites that line the walls of the pores in dehydrated HKUST-1. At both temperatures, there is about 2.21 mmol  $g^{-1}$  that is not desorbed when the pressure of NO is reduced to almost zero. This corresponds to  $\sim 1$  NO per dicopper(II) tetracarboxylate building block for HKUST-1. The results indicate that HKUST-1 is potentially a very good storage material for NO, with a very high capacity compared to those of zeolites and organic polymers.

### IR studies

The dehydrated form of HKUST-1 has accessible copper sites in the walls of the framework itself. Given the well-known tendency of NO to form metal coordination complexes, it seems likely that the hysteresis seen in the adsorption–desorption isotherms of NO on HKUST-1 (Figure 3) is due to trapping of the gas on the metal. Infrared spectroscopy is the technique of choice for probing such bond formation in these solids.

Figure 4 reports the effect NO interaction at room temperature on HKUST-1 monitored by IR spectroscopy. The IR spectrum of a dehydrated HKUST-1 sample is reported in red. The two sharp bands at 1912 and 1886  $cm^{-1}$  are due to overtones and combination modes of framework vibrations, while the 1750–1200  $cm^{-1}$  region is dominated by very intense bands due to asymmetric and symmetric modes of carboxylate (Raman doublet at 1550 and 1460  $cm^{-1}$ ), bands due to benzene ring stretching modes and C–H bending vibrations.<sup>36</sup>

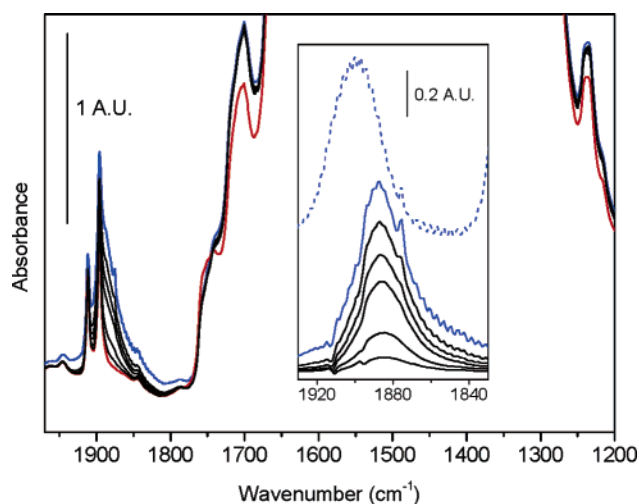


**Figure 4.** Interaction with NO monitored by IR spectroscopy. Red curve: HKUST-1 outgassed at 180 °C. Blue curve: effect of 30 Torr of NO. Black curves: effect of increasing pumping, residual pressure  $10^{-3}$  Torr. (Inset) Background-subtracted spectra in the region of NO stretching (same color code). In the upper part of the inset (blue dashed curve) the spectrum of NO adsorbed at room temperature on a Cu–ZSM-5 zeolite is reported for comparison.

Upon contact with 30 Torr of NO, (blue curve) the growth of a new component at 1887  $cm^{-1}$  is clearly visible, testifying to the formation of a Cu(II)–NO adduct. In the meantime some further changes are observed in the framework modes of HKUST-1, suggesting that the material responds to the NO adsorption. In particular, we observe the erosion of a shoulder at 1755  $cm^{-1}$ , the parallel growth of a component at 1735  $cm^{-1}$  (isobestic point at 1745  $cm^{-1}$ ), and the intensity increase of the bands at 1700 and at 1237  $cm^{-1}$ . The effect of progressive outgassing is reported with black curves. The last spectrum is obtained after outgassing for 15 min at room temperature in dynamic vacuo with a residual partial pressure of  $10^{-3}$  Torr.

The spectroscopic features of NO adsorbed on Cu(II) species are better illustrated in the inset of Figure 4 (same color code) where difference spectra are reported. The Cu(II)–NO adduct is characterized by a band at 1887  $cm^{-1}$  that decreases in intensity without substantial shifts. A  $\Delta\nu(\text{NO}) = +11$   $cm^{-1}$  with respect to  $\nu_{\text{NO}}$  in the gas phase ( $\nu_{\text{N-O}}^0 = 1876$   $cm^{-1}$ ) is close to what has been obtained in case of Cu(II)–NO complex in copper-exchanged zeolites and similar systems,<sup>37–39</sup> where a band in the range 1910–1880  $cm^{-1}$  has been observed. For sake of comparison the spectrum obtained at room temperature on a Cu(ZSM-5) is reported as dashed blue curve in the inset of Figure 4.<sup>38</sup>

Spectroscopic data on copper nitrosyl complexes have been obtained by Zhou et al.<sup>40</sup> They have studied the formation of Cu(NO), [Cu(NO)]<sup>+</sup>, and [Cu(NO)]<sup>−</sup> in neon matrices,<sup>40,41</sup> finding a strong similarity between the spectroscopic features of [Cu(NO)]<sup>+</sup> species (1907.8  $cm^{-1}$ ) and that obtained in the case of Cu(II)-exchanged zeolites. In particular, it has been observed that the N–O stretching frequency reported for Cu-

(36) Prestipino, C.; Regli, L.; Vitillo, J. G.; Bonino, F.; Damin, A.; Lamberti, C.; Zecchina, A.; Solari, P. L.; Kongshaug, K. O.; Bordiga, S. *Chem. Mater.* **2006**, *18*, 1337.

(37) Bordiga, S.; Pazè, C.; Berlier, G.; Scarano, D.; Spoto, G.; Zecchina, A. *Catal. Today* **2001**, *70*, 91.

(38) Lamberti, C.; Bordiga, S.; Salvalaggio, M.; Spoto, G.; Zecchina, A.; Geobaldo, F.; Vlaic, G.; Bellatreccia, M. *J. Phys. Chem. B* **1997**, *101*, 344.

(39) Llabrés i Xamena, F. X.; Fiscaro, P.; Berlier, G.; Zecchina, A.; Turnes Palomino, G.; Prestipino, C.; Bordiga, S.; Giamello, E.; Lamberti, C. *J. Phys. Chem. B* **2003**, *107*, 7036.

(40) Zhou, M.; Andrews, L. *J. Phys. Chem. A* **2000**, *104*, 2618.

(41) Andrews, L.; Citra A. *Chem. Rev.* **2002**, *102*, 885.

(II)–NO/zeolite is near  $1900\text{ cm}^{-1}$ , a value very close to that observed for  $[\text{Cu}(\text{NO})]^+$ , which suggests a +1.0 net charge on the Cu(NO) center for this formal Cu(II)–NO/zeolite species. The  $\text{Cu}(\text{NO})^+$  complex has been described in an ab initio study by Thomas et al.<sup>42</sup> who calculated a binding energy of 91 kJ/mol.

A strong interaction energy and the fact that  $\nu(\text{NO})$  in the Cu(II)–NO adduct appears only slightly shifted from that of the molecule in the gas phase can be explained by considering that the observed frequency is the final result of competitive effects: (i) the polarization effect and  $\sigma$  donation that give an upward shift and (ii) the  $\pi$  back-donation that gives the opposite effect. The fact that the  $\nu(\text{NO})$  in the Cu(II)–NO adduct formed in HKUST-1 is at lower frequency than that observed in Cu–ZSM-5 suggests that in this case the back-donation is more effective. This fact is in agreement with the qualitative observation that the stability of the Cu(II)–NO adducts formed in Cu–ZSM-5 is lower (complete reversibility at room temperature) than that found in HKUST-1. A dedicated study to obtain more quantitative data about the stability of the complex Cu(II)–NO formed in HKUST-1 is in progress.

### Quantification of NO Release

Of course, to make use of a material as a gas storage medium does not just entail being able to adsorb large quantities of the gas but to be able to control the release of the gas at the time and at the rate required for the particular application. The optimum rate of release of NO differs, depending on the exact nature of the target application. For example, for antithrombotic applications the rate of release of NO required should approximate the rate released by the endothelial cells that line the blood vessels in mammals. This rate is quite slow, relating to around  $1\text{ pmol min}^{-1}\text{ mm}^{-2}$ .<sup>9</sup> On the other hand it seems that the antibacterial effects of NO require greater flux of the gas. In our work on zeolites we have shown that exposure of the NO-loaded material to a nucleophile such as water triggers release of the NO. The standard method of measuring NO release from a powdered solid is to expose the material to a flow of wet gas at a controlled relative humidity and measure the NO in the outlet stream using the intensity of chemiluminescence on reaction of NO with ozone. Such experiments carried out on NO-loaded HKUST-1 (Figure 5) indicate that NO is released on contact with water vapor in a manner similar to that seen previously for zeolites. However, the total amount of NO released is 2 orders of magnitude less ( $2\text{ }\mu\text{mol NO per g of HKUST-1}$ ) than the amount initially adsorbed. This is not necessarily a detrimental property as biological applications can require only a very low flux of NO, and we show below that this release of NO is sufficient to completely inhibit platelet aggregation in biological experiments. The total amount of NO released is also significantly less than that seen for zeolites or NONOate polymers but is comparable to the amount of NO released by metal-containing polymers.

### Bioactivity of NO-Loaded HKUST-1

The need for improvements in the biocompatibility of materials is a very important target. This is particularly true for

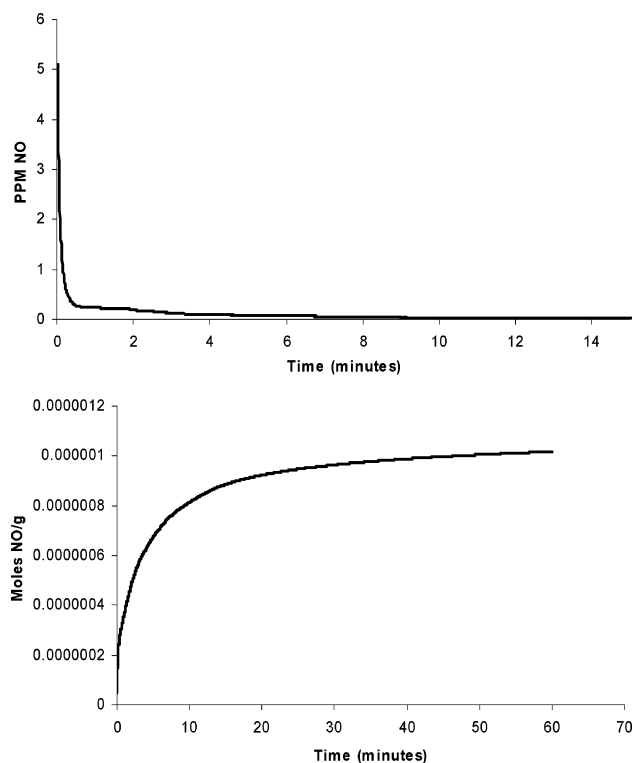


**Figure 5.** NO release profile for NO-loaded HKUST-1 (top) and the cumulative NO released per g of HKUST-1 (bottom).

blood-contacting solids that are used in vascular grafts and in extracorporeal tubing used in coronary bypass surgery and kidney dialysis. Life-threatening complications can occur if thrombosis formation (platelet aggregation and adhesion) is induced by artificial materials that are in contact with blood. Thrombus formation in healthy circulatory systems is inhibited in a number of ways, including the production of small quantities (approximately  $1\text{ pmol min}^{-1}\text{ mm}^{-2}$ ; see reference 9) of NO by the endothelial cells that line the blood vessels and also by platelets. A potentially important strategy for reducing postoperative complications is to make medical devices out of a NO-releasing material, thereby mimicking the antithrombotic action of the endothelial cells.

To overcome the problem of the nondispersion of powders in the liquid-phase, samples of HKUST-1 were prepared as pressed disks with small amounts of poly(tetrafluoroethylene) (PTFE) polymer as a binder. The NO-loaded disks were stored under an inert atmosphere for up to several weeks before being used in further experiments.

The HKUST-1/PTFE disks were suspended by a stainless steel wire holder below the surface of platelet-rich plasma (PRP) in the cuvette of a four-channel platelet aggregometer (Chronolog, Labmedics, Stockport, UK) at  $37\text{ }^\circ\text{C}$ . After a short induction period (1 min), platelet aggregation was initiated using the pro-aggregatory agent, collagen ( $2.5\text{ }\mu\text{g mL}^{-1}$ ), and then measured as a change in turbidity (light transmission) of PRP against a platelet-poor plasma (PPP) reference. Figure 6 shows that a NO-loaded HKUST-1/PTFE sample completely inhibits platelet aggregation. Addition of the NO-scavenger, oxyhemoglobin ( $40\text{ }\mu\text{M}$ ), prevents the inhibitory effect, confirming the central role for NO in the inhibitory process and excluding the possibility that the effects of the NO–HKUST-1 were merely cytotoxic. Furthermore, a control consisting of only HKUST-1

(42) Thomas, J. L. C.; Bauschlicher, C. W., Jr.; Hall, M. B. *J. Phys. Chem. A* **1997**, *101*, 8530.

(43) *Lange's Handbook of Chemistry*, 15th ed.; McGraw-Hill: New York, 1999.

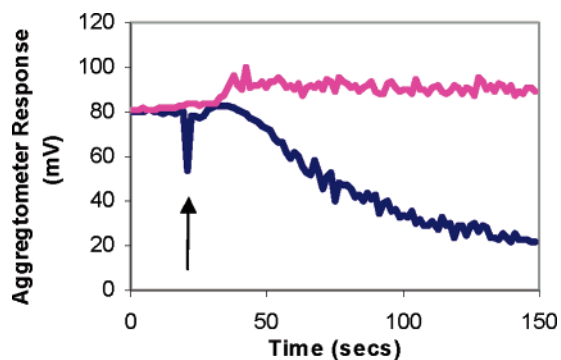


**Figure 6.** Platelet aggregation experiments show that this material inhibits platelet aggregation completely. (Pink = NO-HKUST-1. Blue = control.) On initiation of aggregation (by addition of collagen marked by the arrow) the aggregometer response for the control (blue) indicates that the platelets have aggregated and fallen out of suspension. However, there is no such response for the NO-loaded HKUST-1 sample (pink). This indicates that the amount of NO released by the HKUST-1 is sufficient to completely inhibit platelet aggregation in this experiment.

without NO failed to inhibit aggregation, ruling out any effect from the material itself. For short term applications NO-loaded HKUST-1 seems very promising for antithrombotic applications in that it releases NO at a suitable rate. Unfortunately, however, its stability in biological solutions is limited. Even after a few hours exposure to platelet-rich plasma, the solution itself began to go green, indicating dissolution of the copper from the framework material. Clearly this is an issue as the toxicological implications of excess coppers ions in, for example, human blood may be enough to prevent application of such materials. Further work in this area is ongoing.

### Concluding Remarks

Metal–organic frameworks, such as HKUST-1, are clearly of interest because of their very high adsorption capacities. The hydrogen adsorption measurements are entirely consistent with other gas adsorption measurements and the crystallographic studies. The relatively weak interaction of hydrogen with the walls of a porous solid means that adsorption is restricted to low temperatures. In addition, other gases may well adsorb more strongly than hydrogen, leading to problems unless the hydrogen is ultrapure. This may be exacerbated in materials such as HKUST-1 where there are open metal sites that will interact strongly with other gases or water. However, for adsorption of gases such as NO that do interact strongly with metals, this may be an advantage. In biological applications, the relatively poor stability of MOFs in physiological solutions, and their rather unstudied toxicology, mean that their undoubted promise needs further development before applications can be found. Having said that, however, it is clear that HKUST-1 is a very high-capacity adsorption material. Both hydrogen and nitric oxide adsorb in high quantities on HKUST-1, confirming their applicability as potential gas storage materials for energy, environmental, and biological applications.

### Experimental Section

**Synthesis of HKUST-1.** In a typical synthesis, 3.0 mmol of Cu(NO<sub>3</sub>)<sub>2</sub>·3H<sub>2</sub>O (0.716 g) and 2.0 mmol of benzene 1,3,5-tricarboxylic acid (0.421 g) were mixed with 12 mL of EtOH/H<sub>2</sub>O (50:50) solution in a Teflon-lined autoclave. The mixture was stirred for 30 min at ambient temperature prior to heating in an oven preheated at 383 K, followed by heating at 383 K for 24 h. After crystallization the autoclave

was naturally cooled down to room temperature. The yield was sonicated for 5–10 min in a solution of EtOH/H<sub>2</sub>O (50:50). Large, turquoise-blue crystals were isolated by Büchner filtration and dried in air for 1 day.

**Gas Adsorption/Desorption Measurements. Gases.** Ultrapure hydrogen (H<sub>2</sub> 99.9999%, H<sub>2</sub>O < 500 ppb, N<sub>2</sub> < 200 ppb, O<sub>2</sub> < 100 ppb, CO + CO<sub>2</sub> < 50 ppb, total hydrocarbons <50 ppb) hydrogen was supplied by Air Products Ltd. Deuterium (99.98% D<sub>2</sub>), nitrogen (99.9995%), and carbon dioxide (99.999%) were supplied by BOC Ltd.

**H<sub>2</sub>/D<sub>2</sub> Purification.** Hydrogen and deuterium were purified using a two-stage process involving adsorption on a zeolite (calcium aluminosilicate (1/16 in. pellets)), at 298 K to remove any water vapor present, and activated carbon (G212, particle size 6 × 12 mesh) at 195 K to remove hydrocarbons and other gas impurities.<sup>33</sup> The impurities were adsorbed under these conditions, while little or no hydrogen or deuterium was adsorbed at 195 K. Both adsorbents were degassed at 700 K prior to use.

**Adsorption Studies for H<sub>2</sub>, D<sub>2</sub>, N<sub>2</sub>, and CO<sub>2</sub>.** The adsorption/desorption characteristics of H<sub>2</sub>, D<sub>2</sub>, N<sub>2</sub>, and CO<sub>2</sub> were studied using a Hiden Isochema Gravimetric Analyzer, which is an ultraclean, ultrahigh-vacuum system with a diaphragm and turbo pumping system. The microbalance had a long-term stability of ±1 μg with a weighing resolution of 0.2 μg. The sample was degassed at 453 K under ultrahigh vacuum (10<sup>-10</sup> bar) until no further weight loss occurred prior to H<sub>2</sub> and D<sub>2</sub> adsorption. The approach to equilibrium was measured in real time using a computer algorithm. The pressure was monitored by three pressure transducers with ranges 0–0.2, 0–10, and 0–100 kPa and maintained at the set point by active computer control of inlet/outlet valves throughout the duration of the adsorption kinetic experiments. The accuracy of the set-point pressure regulation was ±0.02% of the range used. Both the sample and counterweight sides of the balance were cooled to 77 K for the H<sub>2</sub> and D<sub>2</sub> adsorption/desorption experiments in order to minimize buoyancy corrections and thermal transpiration effects. A detailed buoyancy correction was carried out on the basis of experimental measurements of the system buoyancy and the helium density of HKUST-1.

The major problem with studying H<sub>2</sub> and D<sub>2</sub> adsorption and desorption is the adsorption of impurities from both the adsorptive gas used and within the UHV system.<sup>33</sup> The measurement protocols used in this study were validated by the complete desorption of H<sub>2</sub> with little or no isotherm hysteresis. More detailed validation of the protocols has been presented previously.<sup>33</sup>

**NO Adsorption/Desorption Measurements.** The adsorption/desorption of NO gas in HKUST-1 was measured using a gravimetric adsorption system. A CI instruments microbalance was thermally stabilized to eliminate the effect from external environment. The microbalance has a sensitivity of 0.1 μg and reproducibility of 0.01% of the load. The pressure of the adsorption system was monitored by two BOC Edwards Active gauges in the ranges of 1 × 10<sup>-8</sup>–1 × 10<sup>-2</sup> and 1 × 10<sup>-4</sup>–1 × 10<sup>3</sup> mbar, respectively. The sample (~130 mg) was initially outgassed at 573 K under 1 × 10<sup>-4</sup> mbar, until no further weight loss was observed. The sample temperature was then decreased to 298 K and kept constant by a circulation water bath with temperature accuracy ±0.02 K. The counterbalance temperature was kept the same as that of the sample to minimize the influence of temperature difference on weight readings, and the sample temperature was monitored using a K type of thermocouple, located close to the sample bucket (<5 mm). The variation in sample temperature was minimal (<0.1 K) throughout the experiment. Nitric oxide gas was introduced into the adsorption system until the desired pressure was achieved, and the mass uptake of the sample was measured as a function of time until the adsorption equilibrium was achieved. In this manner an adsorption isotherm was collected by incrementally increasing the pressure and noting the mass gain of the sample after equilibrium was reached. The desorption of nitric oxide gas adsorbed in the samples was performed by gradually decreasing the system pressure to a desired value (until 2 × 10<sup>-2</sup> mbar).

**Saturated Vapor Pressures.** Hydrogen, deuterium, and nitric oxide were used above their critical temperatures. The saturated vapor pressures for carbon dioxide and nitrogen were calculated using the following equation<sup>44</sup>

$$\log_{10} p = A - \frac{B}{T + C} \quad (1)$$

where  $p$  is the saturated vapor pressure (Torr),  $T$  is the temperature in degrees Celsius and  $A$ ,  $B$ , and  $C$  are constants defined by the adsorbate: carbon dioxide (77–303 K):  $A = 7.810237$ ,  $B = 995.7048$ ,  $C = 293.4754$ ; nitrogen (75–373 K):  $A = 6.49457$ ,  $B = 255.68$ ,  $C = 266.550$ .

**IR Studies.** IR spectra were collected, at  $2 \text{ cm}^{-1}$  resolution, on a Bruker IFS 66 FTIR instrument equipped with a cryogenic MCT detector in transmission mode on a self-supported pellet. Suitable measurements cells were used allowing in situ thermal treatments at  $180 \text{ }^\circ\text{C}$  in high vacuo and NO dosage at room temperature.

**Quantification of NO Release by Chemiluminescence.** Nitric oxide measurements were performed using a Sievers NOA 280i chemiluminescence Nitric Oxide Analyzer. The instrument was calibrated by passing air through a zero filter (Sievers,  $<1$  ppb NO) and 89.48 ppm NO gas (Air Products, balance nitrogen). The flow rate was set to 200 mL/min with a cell pressure of 8.5 Torr and an oxygen pressure of 6.1 psig. To measure NO release from HKUST powders, nitrogen gas of known humidity was passed over the powders, the resultant gas was directed into the analyzer, and the concentration of NO in ppm or ppb was recorded.

**Platelet Aggregation.** The sample of HKUST-1 was ground with PTFE in the desired ratio (75% zeolite/25% PTFE). The mixture was

then pressed into disks (5 mm diameter,  $\sim 20$  mg) under 2 tons for 30 s. The disks were then dehydrated and loaded with nitric oxide as described for the powder samples.

Venous blood was drawn from the antecubital fossa of a healthy volunteer into citrated tubes (0.38% final concentration). The volunteer had not taken any medication known to affect platelet aggregation within the last 10 days. Platelet-rich plasma (PRP) was obtained from whole blood by centrifugation (350g; 20 min; room temperature). Platelet-poor plasma (PPP) was obtained by further centrifugation of PRP (1200g; 5 min; room temperature).

The HKUST-1/PTFE disks were suspended in a stainless steel wire holder below the surface of the PRP in the aggregometer cuvette, ensuring that they did not interfere with the light beam or the mechanical stirring (1000 rpm). After a short incubation period (1 min), platelet aggregation was initiated by addition of agonist collagen ( $2.5 \mu\text{g/mL}$ ). Aggregation was measured as a change in turbidity (light transmission) of PRP against a PPP blank.

**Acknowledgment.** P.S.W. and R.E.M. thank the Leverhulme Trust for support and R.E.M. thanks the Royal Society for the Provision of a University Research Fellowship. We also thank the E.P.S.R.C for support. The friendly and stimulating discussion with Carlo Lamberti and Adriano Zecchina (University of Torino) is gratefully acknowledged.

**Supporting Information Available:** Experimental details. This material is available free of charge via the Internet at <http://pubs.acs.org>.

JA066098K